

# Crustal structure and upper mantle stratigraphy of the Arabian shield

M. Ravi Kumar,<sup>1</sup> D. S. Ramesh,<sup>1</sup> Joachim Saul,<sup>2</sup> Dipankar Sarkar,<sup>1</sup> and Rainer Kind<sup>2</sup>

Received 7 December 2001; revised 28 February 2002; accepted 20 March 2002; published 27 April 2002.

[1] Analysis of receiver functions from an eight-station network on the Saudi Arabian shield indicates that the Moho depths vary between 35–38 km. The crust appears to be rather felsic in nature as evidenced by Poisson's ratios of 0.25–0.27. A prominent negative phase following the Moho conversion is suggestive of a zone of velocity inversion. Indication of mantle stratification is observed beneath the coastal region of Arabia, by way of an additional upper mantle discontinuity at about 240 km. The conversions from the 410 and 660-km discontinuities are significantly delayed, suggesting a slow and hot upper mantle. **INDEX TERMS:** 7205 Seismology: Continental crust (1242); 7218 Seismology: Lithosphere and upper mantle

## 1. Introduction

[2] The Arabian shield occupies the western part of the Arabian plate and appears to be relatively stable amidst the vibrant geodynamic setting of the Middle East. This Precambrian region evolved primarily during the late Proterozoic [Stein and Goldstein, 1996] when it was subjected to episodic reactivation. Since the Pan-African orogeny little tectonic activity has occurred until the start of formation of the Red Sea rift 30–20 Ma ago. Associated with the rifting process, a thin veneer of basalt covers large areas along the western border of the region. The western Arabia region is also characterised by topographic highs of the order of 1000 m and such a buoyant nature is thought to be tied to the presence of hot, low dense upper mantle due to an upwelling mantle plume that currently erodes the overlying lithosphere [Camp and Roobol, 1992]. Results from surface wave dispersion and attenuation measurements using recent broadband observations [Cong and Mitchell, 1998] suggest the presence of crustal fluids that is explained invoking the above hypothesis. Available seismic refraction data in the Arabian shield region [Mooney *et al.*, 1985; Mechie *et al.*, 1986] bring out the presence of a thick (38–44 km) crust.

[3] Although most of the available results seem to suggest the presence of a hot, deforming mantle beneath the Arabian shield, geochemical analysis of peridotite xenoliths and their Sm-Nd ages testify to the relatively chemically inert and isolated nature of the underlying mantle [Stein and Goldstein, 1996]. It is thus uncertain whether this relatively young shield (late Proterozoic) is underlain by a stable lithosphere or a warm deforming mantle.

[4] In this study, we estimate the average crustal Poisson's ratio and investigate upper mantle structure, in the light of the conflicting hypotheses with regard to the tectonic history of the Arabian shield evolution.

## 2. Data and Method of Analysis

[5] Data from an eight station PASSCAL temporary broadband network (Figure 1) in the Arabian shield have been used in this

study. Except for station RIYD situated on sediments, all stations were sited on crystalline basement rock. Details of the Arabian shield station network are presented in Sandvol *et al.* [1998] and Wolfe *et al.* [1999]. Due to possible calibration errors in the vertical component of station RIYD [Laske and Cotte, 2001], we discard it from our analysis.

[6] The method we followed involves rotation of all three axes into a ray coordinate system to decompose the wavefield into its P, SV and SH components [Vinnik, 1977]. The converted phases are isolated from the coda by deconvolving the P from the SV component by simple spectral division in the frequency domain. The deconvolution involves a water level stabilization and additional low pass filtering with a gauss function, which limits the frequency band to that of the data, and suppresses high-frequency noise. In order to make recordings at different slownesses comparable, we apply a moveout correction that reduces the receiver functions to a fixed slowness of 6.4 s/°, corresponding to an epicentral distance of 67°.

[7] The stacked receiver functions for the seven stations (Figure 2), moveout corrected for converted phases, show sharp Moho conversions (Pms) with the corresponding P and S multiples (Ppms and Psms), conversions from weak intra-crustal boundaries and a distinct negative phase following the Pms phase.

[8] The Moho depth  $z_M$  and average crustal Poisson's ratio  $\sigma$  at each location are determined, following the approach of Zhu and Kanamori [2000] (Figure 3). This scheme performs a grid search over the  $\sigma$ - $z_M$  space, in order to determine that  $\sigma$ - $z_M$  pair which best explains the observed Moho conversion and its P and S multiples. The clear Moho multiples resulted in well constrained estimates of  $\sigma$  and  $z_M$  beneath all the stations.

[9] To investigate possible differences in the lithospheric structure and disposition of the 410-km and 660-km discontinuities beneath the shield and the coastal stations close to the Red Sea rift, we construct respective composite sections of receiver functions after filtering them using a low gauss parameter of 1 Hz (Figure 4). We invert their summations to explain the negative phase following the Moho conversion.

## 3. Results and Discussion

### 3.1. Crustal Structure

[10] The results of crustal structure analysis in the Arabian shield are summarized in Table 1. The  $z_M$  values are largely dependent on the average crustal P-velocities considered and therefore uncertainties could be of the order of 2 km. Our crustal thickness estimates (mostly 35–38 km) appear to be on the slightly lower side of the range of values (mostly 40 km and more) observed on a global scale for Proterozoic terrains [Durrheim and Mooney, 1991]. The average Poisson's ratio of the crust yields values in the range 0.251–0.267  $\pm$  0.01 (Figure 3, Table 1). The crustal parameters obtained for the Arabian shield are comparable with those from the Archean Tanzania craton, with average elevations close to 1000 m, as in the present study region. The Tanzanian results show crustal thickness values in the range of 36–42 km with  $\sigma$  values between 0.24–0.26 [Last *et al.*, 1997]. Based on these Poisson's ratios the composition of the Tanzania crust was inferred to be felsic to intermediate. Recent results from the

<sup>1</sup>National Geophysical Research Institute, Hyderabad, India.

<sup>2</sup>GeoForschungsZentrum Potsdam (GFZ), Potsdam, Germany.

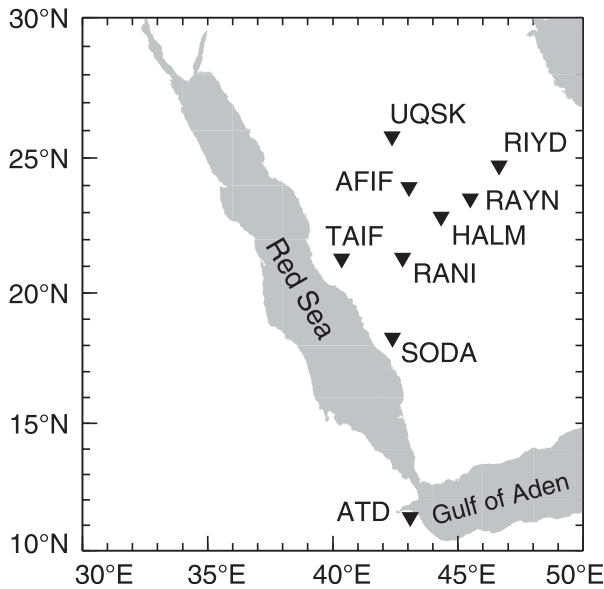


**Figure 1.** Location of the seismic stations used in this study, along with the GEOSCOPE station ATD.

predominantly Precambrian Indian shield [Saul *et al.*, 2000; Kumar *et al.*, 2001] also show rather uniform Poisson's ratios close to 0.25. These lower values from both Archean and Proterozoic shields, comparable among themselves, might in fact be more characteristic of Precambrian shields than the higher value of 0.29 of Zandt and Ammon [1995]. They are also more consistent with the average continental crust composition estimates of Rudnick and Fountain [1995] showing 59% silica content. Further, similar Poisson's ratios for the Proterozoic Arabian shield and the predominantly Archean shields of India and Tanzania suggest that the Poisson's ratio does not increase with crustal age.

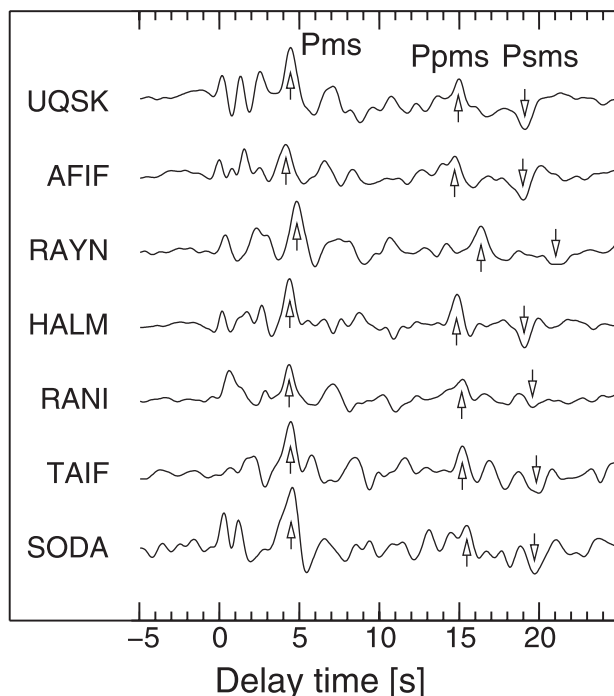


**Figure 2.** Moveout corrected and stacked receiver functions for different stations.

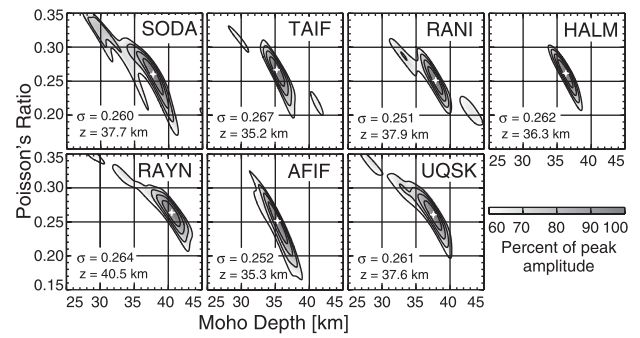


**Figure 3.** Average crustal Poisson's ratio ( $\sigma$ ) and Moho depth ( $z_M$ ) estimation using a grid search scheme.

[11] Earlier refraction results [Mooney *et al.*, 1985; Mechie *et al.*, 1986] and receiver function analysis [Sandvol *et al.*, 1998] bring out the presence of a simple, about 40 km thick crust beneath the Saudi Arabian shield. The crustal thickness obtained here for most of the stations revolves around 35–38 km, indicating the absence of a deep crustal root that is normally expected to be associated with topographic highs. Thus questions are raised as to what sustains such large buoyancy that is manifested in an average elevation of 1000 m in the region.

### 3.2. Upper Mantle Discontinuities

[12] A striking feature in the receiver function sections (Figures 2 and 4) is a pronounced negative phase that immediately follows the Moho conversion seen at around 4.5 s. Inversion of stacked traces shows that this phase can be modelled by a velocity inversion below the Moho (Figure 5). The shear wave attenuation models of Cong and Mitchell [1998] also indicate a zone of high attenuation below the Moho, which they interpret in terms of high temperatures due to a heat source in the upper mantle.

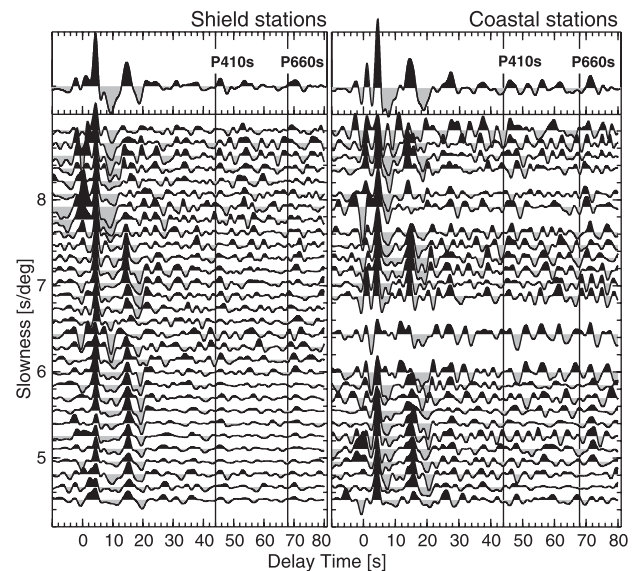


**Figure 4.** Moveout corrected receiver functions, averaged over narrow slowness bins, depicting the crust and upper mantle discontinuities beneath the shield and the coastal regions. The summation of all the traces is shown on top. The vertical lines correspond to P410s and P660s times predicted by the IASP91 model.

**Table 1.** Summary of the Crustal Configuration

Station	Num. Events	Pms(s)	$\sigma$	$z_M$ (km)
SODA	75	4.60	0.260	37.5
TAIF	16	4.55	0.267	35.0
RANI	43	4.40	0.251	38.0
HALM	83	4.45	0.262	36.0
RAYN	33	4.90	0.264	40.0
AFIF	62	4.20	0.252	35.0
UQSK	55	4.50	0.261	37.5

[13] A delay-and-sum technique [Vinnik, 1977; Stammer *et al.*, 1992] has been applied to the traces in Figure 4 to facilitate identification of real conversion phases from upper mantle discontinuities. A series of trial conversion depths are selected to correct the moveout times. For each depth, delay time differences of converted phases between earthquakes with different epicentral distances and a reference epicentral distance are calculated. Receiver functions are shifted to correct for these time differences and stacked (Figure 6). Any enhanced phase that has a reasonable correspondence to the phasing depth and delay time, qualifies for a converted phase.

[14] The coastal stations possibly indicate a coherent phase at a delay time of about 27 s (Figure 4). Also in Figure 6, an enhancement of amplitudes for the coastal stations is observed reasonably clearly at about the same delay time corresponding to a depth of 240 km. In the shield region, the presence of this phase at about 26 s (Figure 4) though not well observed, cannot be ruled out. This signal is thereby interpreted as a converted phase from an interface at approximately 240 km, although the second multiple of the negative phase seems to slightly interfere with P240s conversion energy. Evidence for an abrupt 2–4% increase in P velocity at about 220 km depth (referred to as the L discontinuity) was found by several workers in diverse regions [Leven *et al.*, 1981; Bostock, 1998] subsequent to the work of Lehmann [1961] on the structure of the upper mantle beneath western Europe. From these studies it emerges that the depth of the L discontinuity varies with tectonic setting [Revenaugh and Jordan, 1991].

[15] An examination of Figure 4 suggests that signals from the globally well-resolved seismic 410-km and 660-km discontinuities are rather weak in the moveout corrected image presented for the shield stations. The 410-km (P410s) and the 660-km (P660s) conversion phases are expected to have delay times around 44 and 68 s, respectively. The conversions from these discontinuities beneath the Arabian shield are clearly delayed, arriving at 45.4 and 69.6 s, respectively. The delay is much larger for the coastal stations, near the Red Sea rift, where the measured delay times are 46.3 s and 71.3 s. To estimate the possible errors in the conversion times, we applied a boot-strap resampling technique.

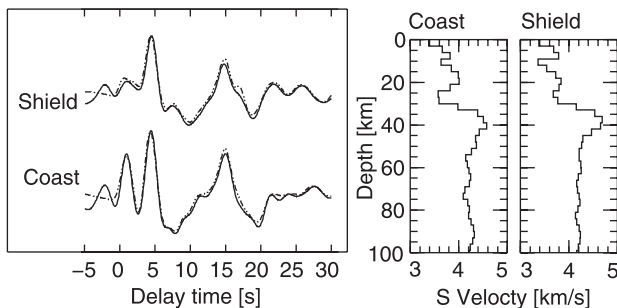


**Figure 5.** Inversion for the negative phase observed after the Moho conversion phase in terms of a negative velocity gradient. Continuous lines are the composite stacked observed receiver functions computed with a Gauss parameter of 1 Hz, and dotted lines indicate the synthetics corresponding to the velocity models.

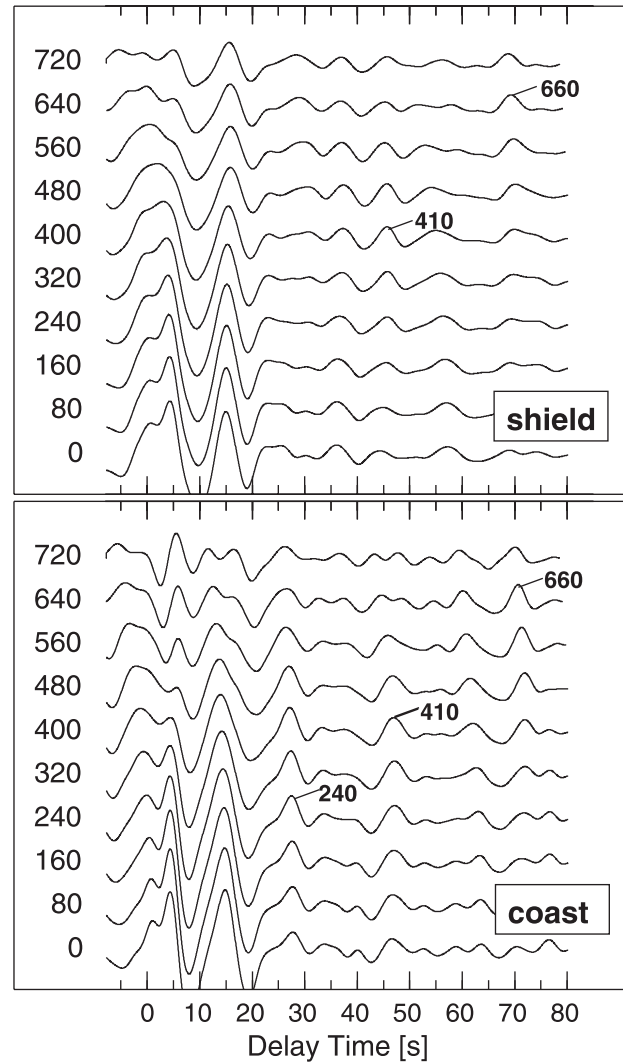


**Figure 6.** Delay-and-sum of the receiver functions in Figure 4. Calculations have been made with reference to an epicentral distance of  $67^\circ$  (corresponding to a slowness of  $6.4 \text{ s}^\circ$ ) for the different phasing depths (km) indicated.

The analysis revealed that the 410 and 660-km discontinuities beneath the shield have the largest uncertainties close to 1.5 and 0.5 s, respectively, whereas for the coast, the respective values are 0.5 and 0.7 s. Similar conversion times for the 410 (47.6 s) and the 660-km (71.9 s) discontinuities have been reported for the station ATD, close to the Red Sea rift [Chevrot *et al.*, 1999]. However, the differential (P660s-P410s) travel time of about 24.5 s, both at the coast and within the shield, is close to the global average of 24 s. This implies that the delay is caused by a slow (hot) mantle above the transition zone and below the Moho, in view of both the normal Poisson's ratio for the crust and normal transition zone thickness. The sub-Moho low velocity gradient zone identified (Figure 5) is likely to contribute to this observed delay.

[16] Global [Zhang and Tanimoto, 1993; Su *et al.*, 1994] and regional studies [Cong and Mitchell, 1998] consistently show low upper mantle velocities beneath the Arabian shield compared to other Precambrian shields. These imply a warm (slow) upper mantle perhaps due to an upwelling plume that currently deforms the Arabian shield mantle [Wolfe *et al.*, 1999]. The presence of late Cenozoic volcanism [Camp and Roobol, 1992] in the region together with the observed topography ( $>1000 \text{ m}$ ) seems to be consistent with the above inferences.

[17] **Acknowledgments.** We thank Lev Vinnik, James Mechie and an anonymous reviewer for their helpful reviews of the manuscript and constructive criticism. Part of the work has been performed under a DLR-CSIR collaboration project.

## References

- Bostock, M. G., Mantle stratigraphy and evolution of the Slave province, *J. Geophys. Res.*, **103**, 21,183–21,200, 1998.
- Camp, V. E., and M. J. Roobol, Upwelling asthenosphere beneath western Arabia and its regional implications, *J. Geophys. Res.*, **97**, 15,255–15,271, 1992.
- Chevrot, S., L. Vinnik, and J. P. Montagner, Global scale analysis of the mantle Pds phases, *J. Geophys. Res.*, **104**(9), 20,203–20,219, 1999.
- Cong, L., and B. J. Mitchell, Seismic velocity and Q structure of the Middle Eastern crust and upper mantle from surface-wave dispersion and attenuation, *Pure Appl. Geophys.*, **153**, 503–538, 1998.
- Durrheim, R. J., and W. D. Mooney, Archaean and Proterozoic crustal evolution: Evidence from crustal seismology, *Geology*, **19**, 606–609, 1991.
- Kumar, M. R., J. Saul, D. Sarkar, R. Kind, and A. K. Shukla, Crustal structure of the Indian shield: New constraints from teleseismic receiver functions, *Geophys. Res. Lett.*, **28**, 1339–1342, 2001.
- Last, R. J., A. A. Nyblade, and C. A. Langston, Crustal structure of the East African Plateau from receiver functions and Rayleigh wave phase velocities, *J. Geophys. Res.*, **102**, 24,469–24,483, 1997.
- Laske, G., and N. Cotte, Surface wave waveform anomalies at the Saudi seismic network, *Geophys. Res. Lett.*, **28**, 4383–4386, 2001.
- Lehmann, I., S and the structure of the upper mantle, *Geophys. J. R. Astron. Soc.*, **4**, 124–138, 1961.
- Leven, J. H., I. Jackson, and A. E. Ringwood, Upper mantle seismic anisotropy and lithosphere decoupling, *Nature*, **289**, 234–239, 1981.
- Mechie, J., C. Prodehl, and G. Koptschalitsch, Ray path interpretation of the crustal structure beneath Saudi Arabia, *Tectonophysics*, **131**, 333–352, 1986.
- Mooney, W. D., M. E. Gettings, H. R. Blank, and J. H. Healy, Saudi Arabian seismic-refraction profile: A travel time interpretation of crustal and upper mantle structure, *Tectonophysics*, **111**, 173–246, 1985.
- Revenaugh, J., and T. H. Jordan, Mantle layering from ScS reverberations 3. The upper mantle, *J. Geophys. Res.*, **96**, 19,781–19,810, 1991.
- Rudnick, R. L., and D. M. Fountain, Nature and composition of the continental crust: A lower crustal perspective, *Rev. Geophys.*, **33**, 267–309, 1995.
- Sandvol, E., D. Seber, M. Barazangi, F. Vernon, R. Mellors, and A. Al-Amri, Lithospheric seismic velocity discontinuities beneath the Arabian shield, *Geophys. Res. Lett.*, **25**, 2873–2876, 1998.
- Stammler, K., R. Kind, N. Petersen, G. Kosarev, L. Vinnik, and Q. Liu, The upper mantle discontinuities: correlated or anticorrelated?, *Geophys. Res. Lett.*, **19**, 1563–1566, 1992.
- Stein, M., and S. L. Goldstein, From plume head to continental lithosphere in the Arabian-Nubian shield, *Nature*, **382**, 773–778, 1996.
- Saul, J., M. R. Kumar, and D. Sarkar, Lithospheric and upper mantle structure of the Indian Shield, from teleseismic receiver functions, *Geophys. Res. Lett.*, **27**, 2357–2360, 2000.
- Su, W.-J., R. L. Woodward, and A. M. Dziewonski, Degree 12 model of shear velocity heterogeneity in the mantle, *J. Geophys. Res.*, **99**, 6945–6980, 1994.
- Vinnik, L. P., Detection of waves converted from P to SV in the mantle, *Phys. Earth Planet. Inter.*, **15**, 294–303, 1977.
- Wolfe, C. J., F. L. Vernon III, and A. Al-Amri, Shear-wave splitting across western Saudi Arabia: The pattern of upper mantle anisotropy at a Proterozoic shield, *Geophys. Res. Lett.*, **26**, 779–782, 1999.
- Zandt, G., and C. J. Ammon, Continental crust composition constrained by measurements of crustal Poisson's ratio, *Nature*, **374**, 152–154, 1995.
- Zhang, Y.-S., and T. Tanimoto, High-resolution global upper mantle structure and plate tectonics, *J. Geophys. Res.*, **98**, 9793–9823, 1993.
- Zhu, L., and H. Kanamori, Moho depth variation in southern California from teleseismic receiver functions, *J. Geophys. Res.*, **105**, 2969–2980, 2000.

M. R. Kumar, D. S. Ramesh, and D. Sarkar, National Geophysical Research Institute, Uppal Road, Hyderabad 500 007, India. (mangalampallyravikumar@rediffmail.com)  
J. Saul and R. Kind, GeoForschungsZentrum Potsdam (GFZ), Telegrafenberg, 14473 Potsdam, Germany. (saul@gfz-potsdam.de)